Journal of the Egyptian Mathematical Society (2014) **22**, 134–142

Egyptian Mathematical Society

Journal of the Egyptian Mathematical Society

www.etms-eg.org
www.elsevier.com/locate/joems

ORIGINAL ARTICLE

Effects of radiation and variable viscosity on unsteady MHD flow of a rotating fluid from stretching surface in porous medium

A.M. Rashad *

Department of Mathematics, Aswan University, Faculty of Science, 81528, Egypt

Received 13 February 2013; revised 7 May 2013; accepted 18 May 2013
Available online 4 July 2013

KEYWORDS

Rotating fluid
Porous medium
Unsteady flow
Variable viscosity
MHD
Thermal radiation

Abstract This work is focused on the study of unsteady magnetohydrodynamics boundary-layer flow and heat transfer for a viscous laminar incompressible electrically conducting and rotating fluid due to a stretching surface embedded in a saturated porous medium with a temperature-dependent viscosity in the presence of a magnetic field and thermal radiation effects. The fluid viscosity is assumed to vary as an inverse linear function of temperature. The Rosseland diffusion approximation is used to describe the radiative heat flux in the energy equation. With appropriate transformations, the unsteady MHD boundary layer equations are reduced to local nonsimilarity equations. Numerical solutions of these equations are obtained by using the Runge–Kutta integration scheme as well as the local nonsimilarity method with second order truncation. Comparisons with previously published work have been conducted and the results are found to be in excellent agreement. A parametric study of the physical parameters is conducted and a representative set of numerical results for the velocity in primary and secondary flows as well as the local skin-friction coefficients and the local Nusselt number are illustrated graphically to show interesting features of Darcy number, viscosity-variation, magnetic field, rotation of the fluid, and conduction radiation parameters.

MATHEMATICS SUBJECT CLASSIFICATION: 76E25; 76N20; 76U05

* Tel.: +20 1014764704.
E-mail address: am_rashad@yahoo.com.
Peer review under responsibility of Egyptian Mathematical Society.

ELSEVIER Production and hosting by Elsevier

1. Introduction

Convective flows in porous media have been extensively studied during the last several decades, and they have included several different physical effects. This interest is due to the many practical applications which can be modeled or approximated

1110-256X © 2013 Production and hosting by Elsevier B.V. on behalf of Egyptian Mathematical Society. Open access under CC BY-NC-ND license.
http://dx.doi.org/10.1016/j.joems.2013.05.008

as transport phenomena in porous media. These flows appear in a wide variety of industrial applications, as well as in many natural circumstances such as geothermal extraction, storage of nuclear waste material, ground water flows, industrial and agricultural water distribution, oil recovery processes, thermal insulation engineering, pollutant dispersion in aquifers, cooling of electronic components, packed-bed reactors, food processing, casting and welding of manufacturing processes, the dispersion of chemical contaminants in various processes in the chemical industry and in the environment, soil pollution, fibrous insulation and even for obtaining approximate solutions for flow through turbo-machinery. This topic is of vital importance in all these applications, thereby generating the need for a full understanding of transport processes through porous media. Theories and experiments of thermal convection in porous media and the state-of-the-art reviews, with special emphasis on practical applications have been presented in the recent books by Ingham and Pop [1], Vafai [2] and Nield and Bejan [3].

Moreover, the magnetohydrodynamic (MHD) rotating fluids in the presence of a magnetic field are encountered in many important problems in geophysics, astrophysics, and cosmical and geophysical fluid dynamics. It can provide explanations for the observed maintenance and secular variations of the geomagnetic field. It is also relevant in the solar physics involved in the sunspot development, the solar cycle, and the structure of rotating magnetic stars. The effect of the Coriolis force due to the Earth's rotation is found to be significant as compared to the inertial and viscous forces in the equations of motion. The Coriolis and electromagnetic forces are of comparable magnitude, the former having a strong effect on the hydromagnetic flow in the Earth's liquid core, which plays an important role in the mean geomagnetic field. Several investigations are carried out on the problem of hydrodynamic flow of a viscous incompressible fluid in rotating medium considering various variations in the problem. Mention may be made of the studies of Ahmed and Sajid [4], Khan and Ellahi [5], Abelman et al. [6], Ellahi et al. [7], Hayat et al. [8], Husain et al. [9] and Hayat et al. [10]. Takhar et al. [11] studied the steady MHD flow and heat transfer on a stretching surface in a rotating fluid. The unsteady flow due to an impulsively stretching surface in a rotating fluid has been considered by Nazar et al. [12]. Hayat et al. [13] studied the hydromagnetic Couette flow of an Oldroyd-B fluid in a rotating system. Hayat et al. [14] investigated the unsteady periodic flows of a magnetohydrodynamic fluid due to noncoxial rotations of a porous disk. Hayat et al. [15] analyzed the effects of Hall current on unsteady flow of a second grade fluid in a rotating system. The steady flow of a rotating third grade fluid past a porous plate has been analyzed by Asghar et al. [16]. Hayat and Mumtaz [17] have examined the resonant oscillations of a plate in an electrically conducting rotating Johnson–Segalman fluid. Hayat [18] has presented the modeling and exact analytic solutions for hydromagnetic oscillatory rotating flows of a Burger's fluid. Abbas et al. [19] studied the unsteady MHD boundary layer flow and heat transfer analysis in an incompressible rotating viscous fluid over a stretching continuous sheet. The problem of free convection heat with mass transfer for MHD non-Newtonian Eyring–Powell flow through a porous medium, over an infinite vertical plate is studied by Eldabe et al. [20]. Mahmoud and Waheed [21] investigated the effects of slip velocity and magnetic field on the flow and heat transfer for micropolar fluid over a permeable stretching surface. Elbashbeshy et al. [22] analyzed the effects of thermal radiation and magnetic field on unsteady mixed convection flow and heat transfer over an exponentially stretching surface.

In all the above studies, the viscosity of the fluid was assumed to be constant. However, it is known that this physical property may change significantly with temperature, and to predict the flow behavior accurately, it may be necessary to take into account viscosity variation for incompressible fluids. Gray *et al.* [23], and Mehta and Sood [24] have found that the flow characteristics substantially change compared with the constant viscosity cases. Ling and Dybbs [25] presented theoretical investigation of temperature-dependent fluid viscosity influence on the forced convection through a semi-infinite porous medium bounded by an isothermal flat plate. EL-Hakiem and Rashad [26] investigated the effect of temperature-dependent viscosity on the non-Darcy natural convection flow over a vertical cylinder saturated porous medium. The problem of heat and mass transfer by non-Darcy free convection adjacent to a vertical cylinder embedded in a saturated porous medium in the presence of thermal radiation effect with temperature-dependent viscosity is considered by Chamkha et al. [27].

The purpose of this work is to generalize the work of Nazar et al. [12] through the inclusion of effects of temperature-dependent viscosity and magnetic field on unsteady MHD boundary layer flow and heat transfer in a rotating fluid due to a stretching surface embedded in a saturated porous medium where the radiation effect is included by invoking the Rosseland diffusion approximation. In formulating the equations governing the flow, a formula for viscosity proportional to an inverse linear function of temperature has been used, following Ling and Dybbs [25]. The parabolic partial differential equations governing the unsteady MHD flow and heat transfer have been solved numerically using the second-level local nonsimilarity method. The second-level local nonsimilarity method is used to convert the nonsimilar equations into a system of ordinary differential equations for the whole transient from initial state ($\xi = 0$) to final steady-state flow ($\xi = 1$). The effects of Darcy number (permeability of porous medium), viscosity-variation, magnetic field, rotation of the fluid, and conduction radiation parameters on the unsteady MHD flow and heat transfer have been presented graphically.

2. Formulation of the problem

Consider the unsteady motion of magnetohydrodynamics-boundary layer flow and heat transfer for a viscous laminar incompressible electrically conducting and rotating fluid due to a stretching surface embedded in a saturated porous medium. At time $t = 0$, the surface coincides with the plane $z = 0$ and it is being stretched the x-direction in a rotating fluid. The fluid is rotating with a constant angular velocity Ω about the z-axis. The flow is three dimensional due to the presence of the Coriolis force. Fig. 1 shows the coordinate system, where u, v, and w are the velocity components in the direction of Cartesian axes x, y and z, respectively. A constant, transverse magnetic field B is applied in the z-direction. Since the flow is induced by stretching the surface in the x-direction only, the velocity components, u, v, w, and the temperature T depends only on x and z. The magnetic Reynolds number $Re_m = \mu_0 \sigma VL$ is assumed to be very small, where μ_0 is the magnetic permeability, σ is the electrical conductivity, and V

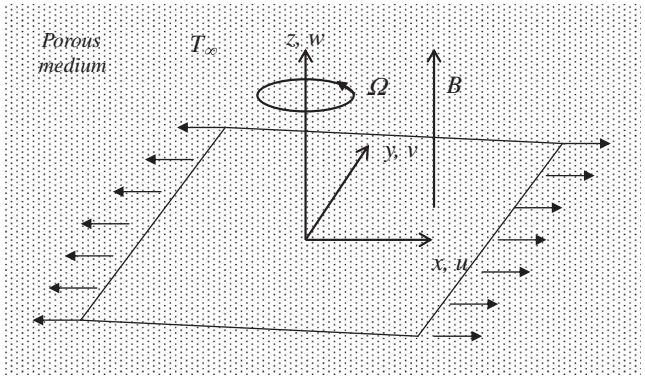

Figure 1 Physical model and coordinate system.

and L are the characteristic velocity and length, respectively. Under these conditions, it is possible to neglect the induced magnetic field in comparison with the applied magnetic field. Since no applied or polarization voltage is imposed on the flow field, the electric field $\vec{E} = \vec{0}$. This corresponds to the case where no energy is added to or extracted from the fluid by electrical means. The surface is electrically insulated. Hence, the Lorenz magnetic force depends only on the magnetic field. The variations of fluid properties are limited and constant, except for the fluid viscosity depends on temperature (see Ling and Dybbs [25]). For the flow in the porous medium, we adopt the Darcy model proposed by Khaled and Vafai [28]. The fluid is considered to be a gray, absorbing-emitting radiation but nonscattering, medium, and the Rosseland approximation is used to describe the radioactive heat flux in the energy equation. The viscous dissipation, Joule heating, and the Hall effect are neglected. The surface temperature and the fluid temperature at the edge of the boundary layer are all constant. Under the foregoing assumptions, the boundary layer equations in the rotating frame of Nazar et al. [12] are given by:

$$\frac{\partial u}{\partial x}+\frac{\partial v}{\partial y}+\frac{\partial w}{\partial z}=0, \tag{1}$$

$$\rho_\infty\left(\frac{\partial u}{\partial t}+u\frac{\partial u}{\partial x}+v\frac{\partial u}{\partial y}+w\frac{\partial u}{\partial z}-2\Omega v\right) = -\frac{\partial p}{\partial x}+\frac{\partial}{\partial z}\left(\mu\frac{\partial u}{\partial z}\right)-\sigma B^2 u-\frac{\mu}{K}u, \tag{2}$$

$$\rho_\infty\left(\frac{\partial v}{\partial t}+u\frac{\partial v}{\partial x}+v\frac{\partial v}{\partial y}+w\frac{\partial v}{\partial z}+2\Omega u\right) = -\frac{\partial p}{\partial y}+\frac{\partial}{\partial z}\left(\mu\frac{\partial v}{\partial z}\right)-\sigma B^2 v-\frac{\mu}{K}v, \tag{3}$$

$$\rho_\infty\left(\frac{\partial w}{\partial t}+u\frac{\partial w}{\partial x}+v\frac{\partial w}{\partial y}+w\frac{\partial w}{\partial z}\right) = -\frac{\partial p}{\partial z}+\frac{\partial}{\partial z}\left(\mu\frac{\partial w}{\partial z}\right)-\frac{\mu}{K}w, \tag{4}$$

$$\rho_\infty C_p\left(\frac{\partial T}{\partial t}+u\frac{\partial T}{\partial x}+v\frac{\partial T}{\partial y}+w\frac{\partial T}{\partial z}\right) = k\frac{\partial^2 T}{\partial z^2}-\frac{\partial q^r}{\partial z}. \tag{5}$$

The initial and boundary conditions are respectively defined as follows:

$$\begin{aligned} &t<0: u(x,y,z,t)=v(x,y,z,t)=w(x,y,z,t)=0,\quad T(x,y,z,t)=T_\infty,\\ &t\geqslant 0: u(x,y,0,t)=ax,\quad v(x,y,0,t)=w(x,y,0,t)=0,\quad T(x,y,0,t)=T_w,\\ &u(x,y,\infty,t)=v(x,y,\infty,t)=w(x,y,\infty,t)=0,\quad T(x,y,\infty,t)=T_\infty, \end{aligned} \tag{6}$$

where p is the pressure, ρ_∞ is the density of the fluid, K is the permeability of porous medium, T is the temperature of the fluid in the boundary layer and the porous medium which are in local thermal equilibrium; T_w is the wall temperature; T_∞ is the ambient temperature. k and C_p are the thermal conductivity and the specific heat at constant pressure, respectively. q^r is the radiative heat flux in the z-direction, where a (>0) is constant and represents the stretching rate.

In addition, the radiative heat flux q^r is described according to the Rosseland approximation such that:

$$q^r=-\frac{4\sigma_1}{3\chi}\frac{\partial T^4}{\partial z}, \tag{7}$$

where σ_1 and χ are the Stefan–Boltzmann constant and the mean absorption coefficient, respectively. As done by Raptis [29], the fluid-phase temperature differences within the flow are assumed to be sufficiently small, so that T^4 may be expressed as a linear function of temperature. This is done by expanding T^4 in a Taylor series about the free-stream temperature T_∞ and neglecting higher-order terms to yield

$$T^4=4T_\infty^3 T-3T_\infty^4, \tag{8}$$

By using Eqs. (6) and (7) in the last term of Eq. (3), we obtain

$$\frac{\partial q^r}{\partial z}=-\frac{16\sigma_1 T_\infty^3}{3\chi}\frac{\partial^2 T}{\partial z^2}. \tag{9}$$

The viscosity of the fluid is assumed to be an inverse linear function of temperature, and it can be expressed as following Ling and Dybbs [25]:

$$\mu=\frac{\mu_\infty}{(1+\gamma(T-T_\infty))}, \tag{10}$$

where γ is a constant and μ_∞ is the viscosity of the ambient fluid. We shall now proceed to transform Eqs. (1)–(5) to a form amenable for numerical solution. To do this, we follow Nazar et al. [12] and introduce the variables:

$$\begin{aligned} &\eta=(a/\upsilon_\infty)^{1/2}\xi^{-1/2}z,\quad u=axf'(\xi,\eta),\quad v=axh(\xi,\eta),\quad w=-(a\upsilon_\infty)^{1/2}\xi^{1/2}f(\xi,\eta),\\ &\xi=1-e^{-\tau},\\ &\tau=at,\quad \upsilon_\infty=\mu_\infty/\rho_\infty,\quad \theta=(T-T_\infty)/(T_w-T_\infty),\quad Da=Ka/\upsilon_\infty,\\ &\lambda=\Omega/a,\quad M=Ha_x^2/Re_x,\quad Ha_x^2=\sigma B^2x^2/\mu_\infty,\quad Re_x=(ax)x/\upsilon_\infty,\quad \theta_r=\gamma(T_w-T_\infty),\\ &\mathrm{Pr}=\mu_\infty C_p/k,\quad R_d=\sigma_1 T_\infty^3/3k\chi. \end{aligned} \tag{11}$$

Substituting variables (11) into Eqs. (2)–(5), we get:

$$\frac{1}{1+\theta_r\theta}f'''-\frac{\theta_r\theta}{(1+\theta_r\theta)^2}f''\theta'-\left(\frac{1}{(1+\theta_r\theta)Da}+M\right)\xi f' +\frac{1}{2}\eta(1-\xi)f''+\xi(ff''-f'^2+2\lambda h) =\xi(1-\xi)\frac{\partial f'}{\partial\xi}, \tag{12}$$

$$\frac{1}{1+\theta_r\theta}h''-\frac{\theta_r\theta}{(1+\theta_r\theta)^2}h'\theta'-\left(\frac{1}{(1+\theta_r\theta)Da}+M\right)\xi h +\frac{1}{2}\eta(1-\xi)h'+\xi(fh'-f'h-2\lambda f') =\xi(1-\xi)\frac{\partial h}{\partial\xi}, \tag{13}$$

$$\frac{1}{\mathrm{Pr}}\left(1+\frac{4R_d}{3}\right)\theta''+\frac{1}{2}\eta(1-\xi)\theta'+\xi f\theta'=\xi(1-\xi)\frac{\partial\theta}{\partial\xi}. \tag{14}$$

where the primes denote the differential with respect to η, f' is the primary flow velocity (i.e., velocity in x direction) and h is

the secondary flow velocity (i.e., velocity in y direction); υ_∞ is the kinematic viscosity at ambient medium, M is the magnetic parameter; Ha is the Hartmann number; Re_x is the local Reynolds number; Da is the Darcy number (permeability of medium); λ is the rotation of the fluid parameter; Pr is the Prandtl number; R_d is the conduction–radiation parameter. Here, θ_r is the viscosity-variation parameter. From (10), it can be seen clearly that the dimensionless viscosity μ/μ_∞ lies in the range $1/(1+\theta_r)$ and 1; its value decreasing with increasing temperature when $\theta_r > 0$. The boundary conditions (6) now become

$$f(\xi,0)=0,\quad f'(\xi,0)=1,\quad h(\xi,0)=0,\quad \theta(\xi,0)=1,$$
$$f'(\xi,\infty)=0,\quad h(\xi,\infty)=0,\quad \theta(\xi,\infty)=0. \tag{15}$$

Eqs. (12)–(14) represent general equations that include various special cases. For example, by formally setting all of M, Da^{-1}, θ_r and R_d equal to 0, Eqs. (9) and (10) reduce to those reported earlier by Nazar et al. [12] in their work concerning unsteady boundary layer flow due to a stretching surface in a rotating fluid. In addition, in the absence of permeability of porous medium $Da^{-1}=0$, thermal radiation effects $R_d=0$, and with constant viscosity $\theta_r=0$.

The quantities of physical interest are the skin friction coefficients and heat transfer coefficient. The local skin friction coefficients in x- and y-directions are given by:

$$C_{fx}=(\mu/\rho_\infty)(\partial u/\partial z)_{z=0}/(ax)^2=Re_x^{-1/2}\xi^{-1/2}(1+\theta_r)^{-1} f''(\xi,0),$$
$$C_{fy}=(\mu/\rho_\infty)(\partial v/\partial z)_{z=0}/(ax)^2=Re_x^{-1/2}\xi^{-1/2}(1+\theta_r)^{-1} h'(\xi,0). \tag{16}$$

Similarly, the local heat transfer coefficient in terms of the local Nusselt number can be expressed as:

$$Nu_x=-x(\partial T/\partial z)_{z=0}/(T_w-T_\infty) = -Re_x^{1/2}\xi^{-1/2}(1+4R_d/3)\theta'(\xi,0). \tag{17}$$

3. Solution

3.1. Initial unsteady solution at $\xi = 0$

For $\xi=0$ (initial unsteady flow), corresponding to $\tau=0$, we have from (12)–(14);

$$\frac{1}{1+\theta_r\theta}f'''-\frac{\theta_r\theta}{(1+\theta_r\theta)^2}f''\theta'+\frac{1}{2}\eta f''=0, \tag{18}$$

$$\frac{1}{1+\theta_r\theta}h''-\frac{\theta_r\theta}{(1+\theta_r\theta)^2}h'\theta'+\frac{1}{2}\eta h'=0, \tag{19}$$

$$\frac{1}{\mathrm{Pr}}\left(1+\frac{4R_d}{3}\right)\theta''+\frac{1}{2}\eta\theta'=0. \tag{20}$$

subject to

$$f(0)=0,\quad f'(0)=1,\quad h(0)=0,\quad \theta(0)=1$$
$$f'(\infty)=0,\quad h(\infty)=0,\quad \theta(\infty)=0. \tag{21}$$

3.2. Steady state solution at $\xi = 1$

For $\xi=1$ (final steady flow), corresponding to $\tau\to\infty$, Eqs. (12)–(14) give

$$\frac{1}{1+\theta_r\theta}f'''-\frac{\theta_r\theta}{(1+\theta_r\theta)^2}f''\theta'-\left(\frac{1}{(1+\theta_r\theta)Da}+M\right)f' + (ff''-f'^2+2\lambda h)=0, \tag{22}$$

$$\frac{1}{1+\theta_r\theta}h''-\frac{\theta_r\theta}{(1+\theta_r\theta)^2}h'\theta'-\left(\frac{1}{(1+\theta_r\theta)Da}+M\right)h + (fh'-f'h-2\lambda f') = 0, \tag{23}$$

$$\frac{1}{\mathrm{Pr}}\left(1+\frac{4R_d}{3}\right)\theta''+f\theta'=0. \tag{24}$$

(24) subject to (21).

3.3. Solution for small ξ (or τ)

A second-level local similarity method introduced by Minkowycz and Sparrow [30] in this case can be used to convert the nonsimilar equations into a system of ordinary differential equations. Introducing new functions $G=\partial f/\partial\xi$, $\omega=\partial h/\partial\xi$ and $\varphi=\partial\theta/\partial\xi$. The second level of truncation Eqs. (12)–(14) can be expressed in the following form:

$$\frac{1}{1+\theta_r\theta}f'''-\frac{\theta_r\theta}{(1+\theta_r\theta)^2}f''\theta'-\left(\frac{1}{(1+\theta_r\theta)Da}+M\right)\xi f' + \frac{1}{2}\eta(1-\xi)f''+\xi(ff''-f'^2+2\lambda h) = \xi(1-\xi)G', \tag{25}$$

$$\frac{1}{1+\theta_r\theta}h''-\frac{\theta_r\theta}{(1+\theta_r\theta)^2}h'\theta'-\left(\frac{1}{(1+\theta_r\theta)Da}+M\right)\xi h + \frac{1}{2}\eta(1-\xi)h'+\xi(fh'-f'h-2\lambda f') = \xi(1-\xi)\omega, \tag{26}$$

$$\frac{1}{\mathrm{Pr}}\left(1+\frac{4R_d}{3}\right)\theta''+\frac{1}{2}\eta(1-\xi)\theta'+\xi f\theta'=\xi(1-\xi)\varphi. \tag{27}$$

Differentiating the above equations with respect to ξ and neglecting the terms involving the derivative functions of G, φ and ω with respect to ξ, one may easily find the following:

$$\frac{1}{1+\theta_r\theta}G'''-\frac{\theta_r}{(1+\theta_r\theta)^2}f'''\varphi-\frac{\theta_r\theta}{(1+\theta_r\theta)^2}(f''\varphi'+G''\theta') -\frac{(1+\theta_r\theta)\theta_r\varphi-2\theta_r^2\theta\varphi}{(1+\theta_r\theta)^3}f''\theta'-\frac{1}{(1+\theta_r\theta)Da}(\xi G'+f') - M(\xi G'+f')+\frac{\theta_r\varphi}{(1+\theta_r\theta)^2Da}\xi f'+\frac{1}{2}\eta(1-\xi)G'' -\frac{1}{2}\eta f''+(ff''-f'^2+2\lambda h)+\xi(f''G+fG''-2f'G' +2\lambda\omega) = (1-2\xi)G', \tag{28}$$

$$\frac{1}{1+\theta_r\theta}\omega''-\frac{\theta_r}{(1+\theta_r\theta)^2}h''\varphi-\frac{\theta_r\theta}{(1+\theta_r\theta)^2}(h'\varphi'+\omega'\theta') -\frac{(1+\theta_r\theta)\theta_r\varphi-2\theta_r^2\theta\varphi}{(1+\theta_r\theta)^3}h'\theta'-\frac{1}{(1+\theta_r\theta)Da}(\xi\omega+h) - M(\xi\omega+h)+\frac{\theta_r\varphi}{(1+\theta_r\theta)^2Da}\xi h+\frac{1}{2}\eta(1-\xi)\omega' -\frac{1}{2}\eta h'+(fh'-f'h-2\lambda f')+\xi(h'G+f\omega'-hG'-f'\omega -2\lambda G') = (1-2\xi)\omega, \tag{29}$$

$$\frac{1}{\Pr}\left(1+\frac{4R_d}{3}\right)\varphi''+\frac{1}{2}\eta(1-\xi)\varphi'-\frac{1}{2}\eta\theta'+f\theta'+\xi(G\theta'+f\varphi')=(1-2\xi)\varphi. \quad (30)$$

subject to

$$f(\xi,0)=0,\quad f'(\xi,0)=1,\quad h(\xi,0)=0,\quad \theta(\xi,0)=1,$$
$$f'(\xi,\infty)=0,\quad h(\xi,\infty)=0,\quad \theta(\xi,\infty)=0,$$
$$G(\xi,0)=0,\quad G'(\xi,0)=0,\quad \omega(\xi,0)=0,\quad \varphi(\xi,0)=0,$$
$$G'(\xi,\infty)=0,\quad \omega(\xi,\infty)=0,\quad \varphi(\xi,\infty)=0. \quad (31)$$

4. Results and discussion

The numerical results for the dimensionless velocity profiles of the rotating fluid in x and y directions, as well as the local skin friction coefficients and the local Nusselt number are obtained using two distinct solution techniques, namely, the fourth order Runge–Kutta scheme and local nonsimilarity methodology having Prandtl number Pr equal to 0.7 (suitable for air), while the representative values of the magnetic parameter M ranging from 0.0 to 2.0, the Darcy number Da ranging from 1.0 to 10^{10} (i.e., ∞), the fluid rotation parameter λ ranging from 0.0 to 1.0, the dimensionless time ξ ranging from 0.0 to 1.0, the viscosity-variation parameter θ_r ranging from 0.0 to 0.4, and the conduction–radiation parameter R_d ranging from 0.0 to 1.0. In order to assess the accuracy of the numerical method, we have compared our numerical results with those of Nazar et al. [12] in the absence of magnetic field, permeability of porous medium, and radiation effects when the fluid viscosity is constant. The comparison is found to be in good agreement was shown in Table 1.

The effect of increase in the viscosity variation parameter θ_r, for different values of magnetic parameter M on the dimensionless velocity profiles in x and y directions ($f'(\xi,\eta)$and $h(\xi,\eta)$), respectively, at the final steady state flow $\xi = 1$ is depicted in Figs. 2 and 3, respectively. Application of a uniform magnetic field in the z-direction to an electrically-conducting fluid gives rise to a flow resistive force called the Lorentz force in both the x- and y-directions, which supports the motion in y direction, but opposes the motion in x direction. This retardation effect is accompanied by an appreciable decrease in values of the velocity profiles in x direction $f'(\xi,\eta)$, but an increase in the values of the velocity profiles in y direction $h(\xi,\eta)$. Moreover, the fluid hydrodynamic boundary layer thickness become thicker as the magnetic parameter M increases. These behaviors are clearly depicted in Figs. 2 and 3. Also, an increase in the viscosity-variation parameter θ_r leads to the decrease in velocity profiles in x-direction, while the opposite behaviors with velocity profiles in y-direction. Thus, the increase in viscosities accelerates the fluid motion in y-direction and reduces it in x-direction along the wall. Moreover, it is seen that the fluid hydrodynamic boundary layer thickness gradually reduces when the viscosity parameter θ_r increases.

Table 1 Comparison for various values of $-f''(0)$ and $-h'(0)$ for various values of λ for ($Da^{-1} = M = R_d = \theta_r = 0$) at $\xi = 1.0$ (final steady-state flow).

Λ	Nazar et al. [12]		Present results	
	$-f''(0)$	$-h'(0)$	$-f''(0)$	$-h'(0)$
0	1.0000	0.000	1.00000	0.0000
0.5	1.1384	0.5128	1.13843	0.51282
1.0	1.3250	0.8371	1.32502	0.83714
2.0	1.6523	1.2873	1.65233	1.28731

The effects of Darcy number Da and the rotation of fluid parameter λ on the velocity in primary and secondary flows $f'(\xi,\eta)$ and $h(\xi,\eta)$ are depicted in Figs. 4 and 5. The presence of porous medium in the flow has the tendency to increase the resistance to the motion of the fluid along the sheet. As the result of this flow behavior, it can be seen that the velocity profiles in x-direction $f'(\xi,\eta)$ increases as the Darcy number Da increases, whereas the opposite behavior happens with the velocity in y-direction $h(\xi,\eta)$. This means that the presence of porous medium causes higher restriction to the fluid, which enhances the primary fluid flow and reduces the secondary of the fluid flow. On other hand, as the rotation of fluid λ increases, the velocity profiles in x-direction decreases, and the decrease in the velocity for large values of λ is oscillatory, while the velocity profiles in y-direction, $h(\xi,\eta)$ increases and both the fluid hydrodynamic boundary layers decrease. This is because the rotation parameter represents the Coriolis force which leads to accelerate the fluid motion. It can be also noticed that for zero and small values of λ, the velocities decay monotonically exponentially, while for large values of λ, the decay is oscillatory ($\lambda = 0$ the flow is governed by Blasius equation).

Figs. 6 and 7 show the effects of varying the conduction–radiation parameter R_d and the dimensionless time ξ on the velocity profiles in x- and y-directions $f'(\xi,\eta)$ and $h(\xi,\eta)$ respectively. Increases in the values of R_d have a tendency to decrease the dimensionless on the velocity profiles in x-direction, whereas the opposite behavior occurs with the velocity profiles in y-direction. This result is expected because the presence of thermal radiation works as a heat source and so the quantity of heat added to the flow causes the motion of the rotating fluid to accelerate. In addition, increases in the value of the radiation parameter R_d cause a slight reduction in the fluid hydrodynamic boundary layer thickness and, hence, in the thermal boundary layer thicknesses. On other hand, it can be seen that increases in the dimensionless time ξ tend to reduce

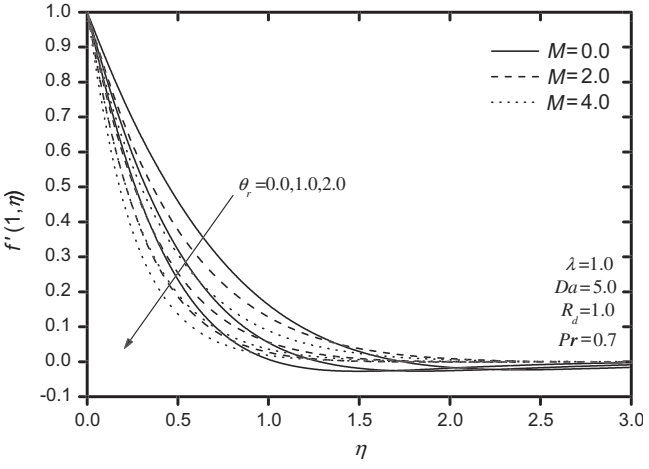

Figure 2 Velocity profiles in x-direction for different values of the viscosity-variation parameter θ_r and magnetic parameter M.

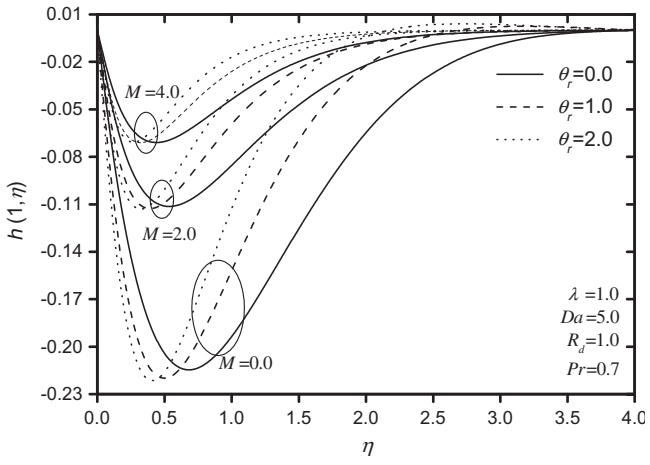

Figure 3 Velocity profiles in y-direction for different values of the viscosity-variation parameter θ_r and magnetic parameter M.

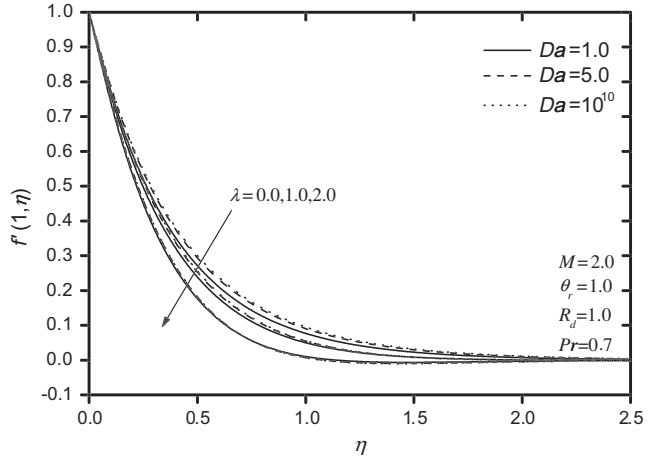

Figure 4 Velocity profiles in x-direction for different values of Darcy number Da and rotation of fluid parameter λ.

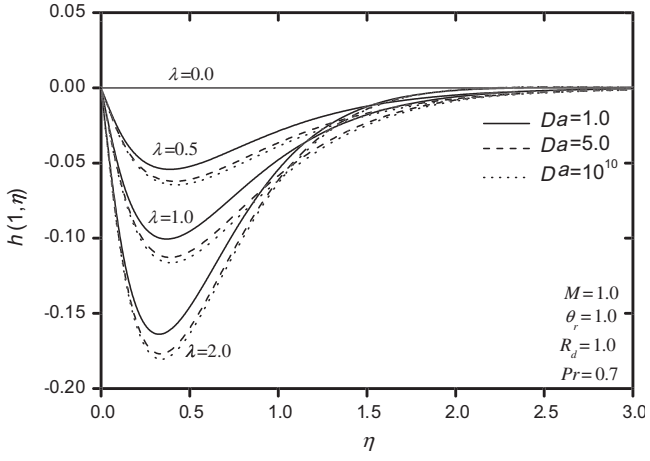

Figure 5 Velocity profiles in y-direction for different values of Darcy number Da and rotation of fluid parameter λ.

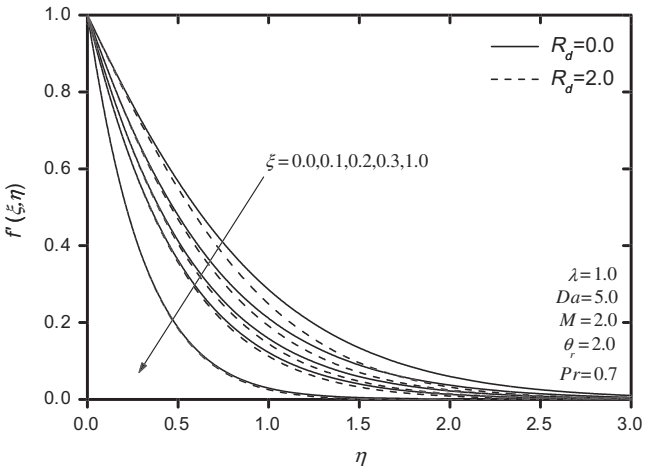

Figure 6 Velocity profiles in x-direction for different values of the conduction–radiation parameter R_d and dimensionless time ξ.

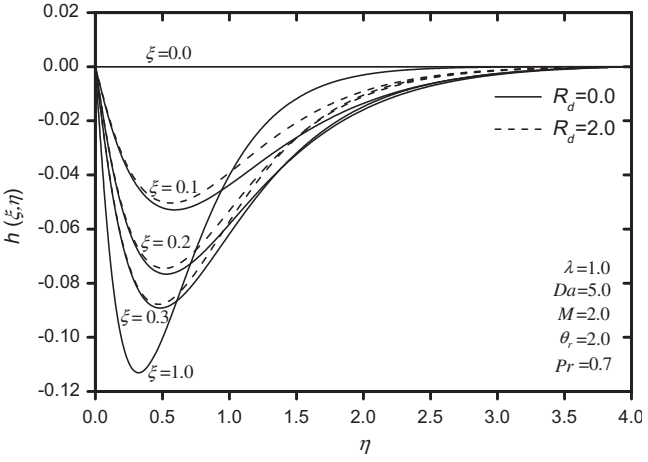

Figure 7 Velocity profiles in y-direction for different values of the conduction–radiation parameter R_d and dimensionless time ξ.

both the velocity profiles in x-and y-directions. This causes a decrease in both the fluid hydrodynamic flow boundary layers thickness in x- and y-directions.

Figs. 8–10 display the variation of the skin friction coefficients in x- and y-directions ($-f''(\xi,0)$ and $-h'(\xi,0)$) and the local Nusselt number $-\theta'(\xi,0)$ with the dimensionless time ξ for various values of the magnetic parameter M and Darcy number Da. It can be seen that the skin friction coefficient in the x-direction increases with the increase in the magnetic parameter M or decreasing the Darcy number Da, whereas the opposite trend occurs with both the skin friction coefficient in the y-direction and the local Nusselt number. The reason for this trend is attributed to the fact that the presence of porous medium represents additional resistance to flow field, thus slowing the fluid flow. This flow resistance has the same effect as that produced by the application of a magnetic field. Moreover, this results in higher skin friction coefficient in x-direction, but lower skin friction coefficient in y-direction.

The effects of the viscosity-variation parameter θ_r, the rotation of fluid parameter λ and the conduction–radiation

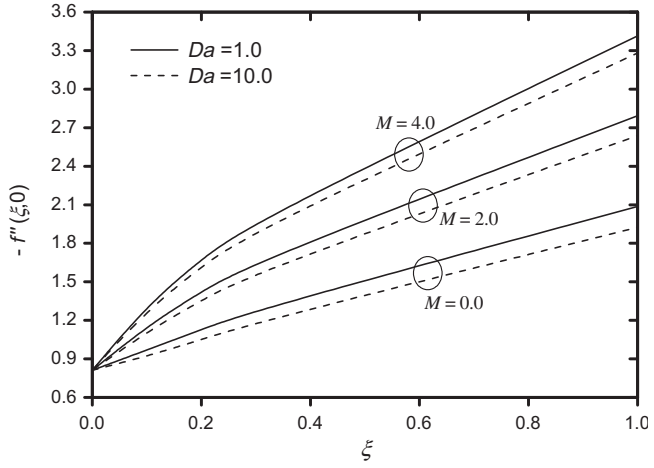

Figure 8 Local skin friction coefficient in x-direction for different values of Darcy number Da and magnetic parameter M.

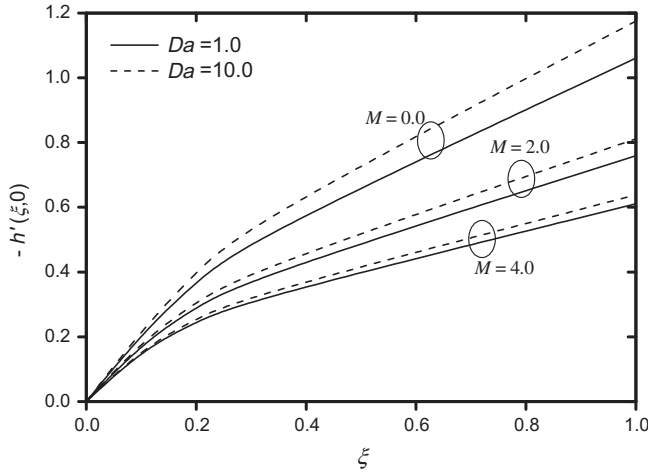

Figure 9 Local skin friction coefficient in y-direction for different values of Darcy number Da and magnetic parameter M.

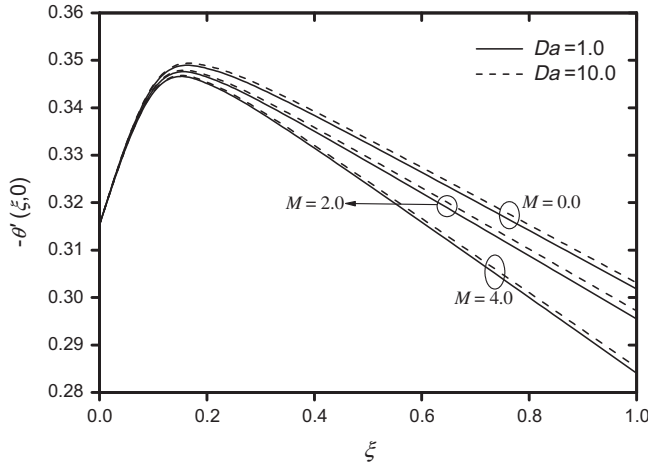

Figure 10 Local Nusselt number for different values of Darcy number Da and magnetic parameter M.

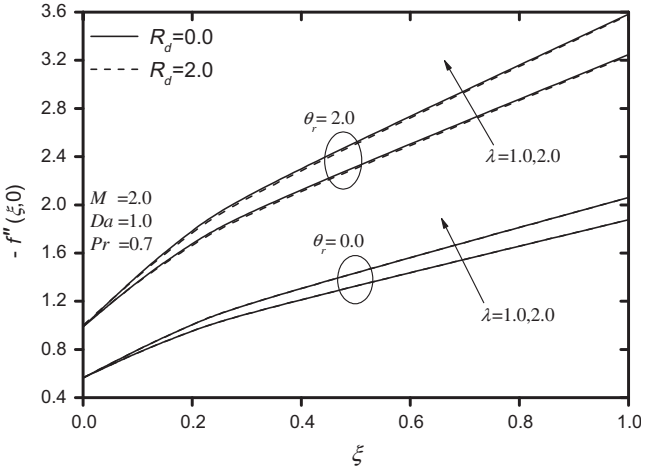

Figure 11 Local skin friction coefficient in x-direction for different values of the viscosity-variation parameter θ_r, rotation of fluid parameter λ, and conduction–radiation parameter R_d.

parameter R_d on the skin friction coefficients and Nusselt number are displayed in Figs. 11–13. An increase in the viscosity variation parameter θ_r leads to an increase in the values of skin friction coefficient in x- and y-directions, while a decrease in the values of the local Nusselt number. This qualitative effect arises because the fluid is able to move more easily close to the sheet surface since its viscosity is lower relative to the constant viscosity case and hence decreased the local Nusselt number. This is an expected result because as the viscosity variation parameter increases, fluid hydrodynamic boundary layer thickness reduces. This causes the value of the wall velocity gradient to increase, whereas the negative values of the wall temperature gradients decrease yielding corresponding decreases in the local skin friction coefficients and increases in the Nusselt number. Furthermore, it can be noticed that an increase in the conduction–radiation parameter R_d leads to a decrease in the skin friction coefficients and the local Nusselt number. This may be attributed to the fact that the increase in the values of R_d produces a reduction in the fluid hydrodynamic boundary layer thickness and hence implies less interaction of radiation with both the momentum and thermal boundary layers. Obviously, for $\theta_r = 0.0$ (the case of a fluid with a constant viscosity), changes in the values of R_d will cause no changes in the profiles of velocity in primary and secondary flows. That is because Eqs. (12) and (13) uncoupled from Eq. (14) at $\theta_r = 0.0$. Finally, as seen earlier from Figs. 4 and 5, it is found that the Coriolis force assists the fluid motion and reduce the hydrodynamic boundary layers which results in an increase in the velocity gradients in the primary and secondary flows and hence in the skin friction coefficients for the primary and secondary flows. Thus, the skin-friction coefficients increase while the local Nusselt number decreases considerably as the rotation parameter λ increases. These behaviors are clearly shown in Figs. 11–13.

5. Conclusions

In this paper, the effects of temperature-dependent viscosity and magnetic field on unsteady MHD boundary layer flow and heat transfer in a rotating fluid due to a radiating stretching surface embedded in a saturated porous medium were

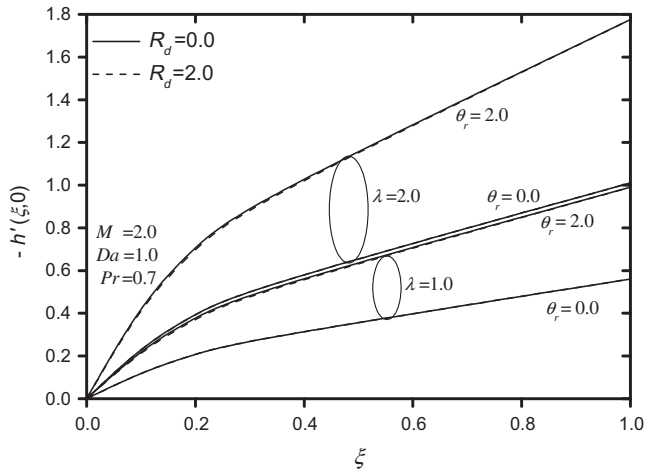

Figure 12 Local skin friction coefficient in y-direction for different values of the viscosity-variation parameter θ_r, rotation of fluid parameter λ, and conduction–radiation parameter R_d.

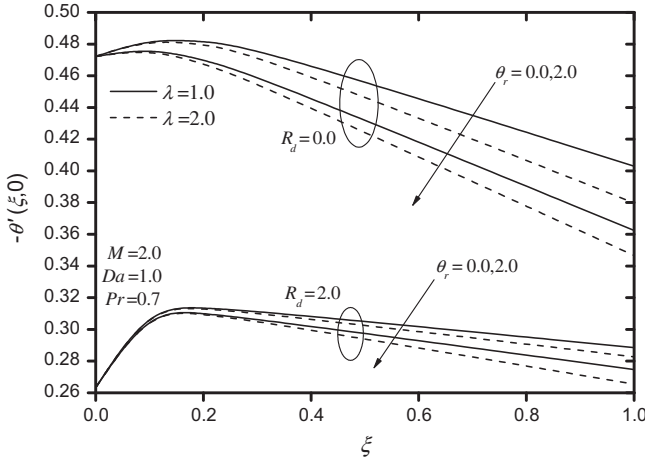

Figure 13 Local Nusselt number for different values of the viscosity-variation parameter θ_r, rotation of fluid parameter λ, and conduction–radiation parameter R_d.

investigated. The fluid viscosity is assumed to vary as an inverse linear function of temperature and the Rosseland diffusion approximation is used to describe the radiative heat flux in the energy equation. Comparison with previously published work was performed, and the results are found to be in excellent agreement. Numerical results for the velocity in primary and secondary flows as well as the local skin-friction coefficients and the local Nusselt number were reported graphically. It has been found that the surface skin-friction coefficient in x-direction and the Nusselt number increase with the increase in magnetic field, but the skin friction coefficient in y-direction decreases, whereas the opposite behaviors were predicted as the Darcy number increases. In addition, the effects of the magnetic field and the permeability of porous medium are more pronounced on the skin friction coefficients than on the Nusselt number. Moreover, it is apparent that decreasing the conduction–radiation parameter enhances the local Nusselt number, whereas it has a weakly effect on the skin-friction coefficients. In addition, the Nusselt number decreases, whereas the skin friction coefficients for both the primary and secondary flows increase significantly with the increase in the rotation parameter, and the skin friction coefficient for the secondary flow is strongly dependent on it. Finally, an increase in the viscosity variation parameter leads to an increase in the values of skin friction coefficient in x- and y-directions, whereas the opposite behavior with the local Nusselt number. It is hoped that the present work will serve as a motivation for future experimental work which seems to be lacking at the present time.

Acknowledgement

The author is very thankful to the reviewers for their constructive comments which have improved significantly the quality of the paper.

References

[1] D. Ingham, I. Pop (Eds.), Transport Phenomena in Porous Media, Oxford, 2005.
[2] K. Vafai (Ed.), Handbook of Porous Media, second ed., Taylor & Francis, New York, 2005.
[3] D.A. Nield, A. Bejan, Convection in Porous Media, third ed., Springer, New York, 2006.
[4] G. Ahmed, Muhammad Sajid, Thin-film flow of MHD third grade fluid in a porous space, J. Porous Media 12 (2009) 65–75.
[5] Masood Khan, R. Ellahi, Exact solution of oscillatory rotating flows of a generalized Oldroyd-B fluid through porous medium.: J. Porous Media. 12 (2009) 777–788.
[6] S. Abelman, E. Momoniat, T. Hayat, Steady MHD flow of a third grade fluid in a rotating frame and porous space, Nonlinear Anal.: Real World Appl. 10 (6) (2009) 3322–3328.
[7] R. Ellahi, T. Hayat, F.M. Mahomed, The analytical solutions for magnetohydrodynamic flow of a third order fluid in a porous medium, Zeitschrift Fur Naturforschung A 64 (9) (2009) 531–539.
[8] T. Hayat, H.M. Mamboundou, F.M. Mahomed, A note on some solutions for the flow of a fourth grade fluid in a porous space, Nonlinear Anal.: Real World Appl. 10 (1) (2009) 368–374.
[9] M. Husain, T. Hayat, C. Fetecau, A note on decay of potential vortex in an Oldroyd-B fluid through a porous space, Nonlinear Anal.: Real World Appl. 10 (4) (2009) 2133–2138.
[10] T. Hayat, R. Naz, M. Sajid, On the homotopy solution for Poiseuille flow of a fourth grade fluid, Commun. Nonlinear Sci. Numer. Simul. 15 (3) (2010) 581–589.
[11] H.S. Takhar, A.J. Chamkha, G. Nath, Flow and heat transfer on a stretching surface in a rotating fluid with a magnetic field, Int. J. Thermal Sci. 42 (2003) 23–31.
[12] R. Nazar, N. Amin, I. Pop, Unsteady boundary layer flow due to a stretching surface in a rotating fluid, Mech. Res. Commun. 31 (2004) 121–128.
[13] T. Hayat, S. Nadeem, S. Asghar, Hydromagnetic couette flow of an Oldroyd-B fluid in a rotating system, Int. J. Eng. Sci. 42 (2004) 65–78.
[14] T. Hayat, R. Ellahi, S. Asghar, Unsteady periodic flows of a magnetohydrodynamic fluid due to noncoxial rotations of a porous disk and a fluid at infinity, Math. Comput. Model. 40 (2004) 173–179.
[15] T. Hayat, S. Nadeem, S. Asghar, A.M. Siddiqui, effects of hall current on unsteady flow of a second grade fluid in a rotating system, Chem. Eng. Commun. 192 (2005) 1272–1284.
[16] S. Asghar, M.M. Gulzar, T. Hayat, Rotating flow of a third grade fluid by homotopy analysis method, Appl. Math. Comput. 165 (2005) 213–221.

[17] T. Hayat, S. Mumtaz, Resonant oscillations of a plate in an electrically conducting rotating Johnson–Segalman fluid, Comput. Math. Appl. 50 (2005) 669–1676.
[18] T. Hayat, Exact solutions to rotating flows of a Burgers' fluid, Comput. Math. Appl. 52 (2006) 1413–1424.
[19] Z. Abbas, T. Javed, M. Sajid, N. Ali, Unsteady MHD flow and heat transfer on a stretching sheet in a rotating fluid, J. Taiwan Inst. Chem. Eng. 41 (2010) 644–650.
[20] N.T.M. Eldabe, Sallam N. Sallam, Mohamed Y. Abou-zeid, Numerical study of viscous dissipation effect on free convection heat and mass transfer of MHD non-Newtonian fluid flow through a porous medium, J. Egyptian Math. Soc. 20 (2012) 139–151.
[21] M.A.A. Mahmoud, S.E. Waheed, MHD flow and heat transfer of a micropolar fluid over a stretching surface with heat generation (absorption) and slip velocity, J. Egyptian Math. Soc. 20 (2012) 20–27.
[22] E.M.A. Elbashbeshy, T.G. Emam, K.M. Abdelgaber, Effects of thermal radiation and magnetic field on unsteady mixed convection flow and heat transfer over an exponentially stretching surface with suction in the presence of internal heat generation/absorption, J. Egyptian Math. Soc. 20 (2012) 215–222.
[23] J. Gary, D.R. Kassory, H. Tadjeran, A. Zebib, The effect of significant viscosity variation on convective heat transport in water-saturated porous media, J. Fluid Mech. 117 (1982) 233–249.
[24] K.N. Mehta, S. Sood, Transient free convection flow with temperature-dependent viscosity in a fluid saturated porous medium, Int. J. Eng. Sci. 30 (1992) 1083–1087.
[25] J.X. Ling, A. Dybbs, Forced convection over a flat plate submersed in a porous medium: variable viscosity case, in: ASME Paper 87-WA/HT-23, ASME Winter Annual Meeting, Boston, Massachusetts, 1987, pp. 13–18.
[26] M.A. EL-Hakiem, A.M. Rashad, Effect of radiation on non-Darcy free convection from a vertical cylinder embedded in a fluid-saturated porous medium with a temperature-dependent viscosity, J. Porous Media 10 (2) (2007) 209–218.
[27] A.J. Chamkha, S.M.M. EL-Kabeir, A.M. Rashad, Heat and mass transfer by non-Darcy free convection from a vertical cylinder embedded in porous media with a temperature-dependent viscosity, Int. J. Numer. Methods Heat Fluid Flow 21 (7) (2011) 847–863.
[28] A.R.A. Khaled, K. Vafai, The role of porous media in modeling flow and heat transfer in biological tissues, Int. J. Heat Mass Transfer 46 (2003) 4989–5003.
[29] A. Raptis, Radiation and free convection flow through a porous medium, Int. Commun. Heat Mass Transfer 25 (1998) 289–295.
[30] W.J. Minkowycz, E.M. Sparrow, Numerical solution scheme for local nonsimilarity boundary-layer analysis, Numer. Heat Trans. 1 (1978) 69–85.